Complex and Hierarchical 2D Assemblies via Crystallization-Driven Self-Assembly of Poly(L-lactide) Homopolymers with Charged Termini

Xiaoming He,[1,2] Yunxiang He,[1] Ming-Siao Hsiao,[3] Robert L. Harniman,[1] Sam Pearce,[1] Mitchell A. Winnik,[4] and Ian Manners[1,*]

[1]School of Chemistry, University of Bristol, Bristol BS8 1TS, United Kingdom

[2]Current Address: School of Chemical Science and Engineering, Tongji University, Shanghai 200092, China

[3]UES, Inc. and Materials & Manufacturing Directorate, Air Force Research Laboratory, Wright-Patterson AFB, OH 45433, USA

[4]Department of Chemistry, University of Toronto, Toronto, Ontario M5S 3H6, Canada

ABSTRACT: Poly(L-lactide) (PLLA)-based nanoparticles have attracted much attention with respect to applications in drug delivery and nanomedicine as a result of their biocompatibility and biodegradability. Nevertheless, the ability to prepare PLLA assemblies with well-defined shape and dimensions is limited and represents key challenge. Herein we report access to a series of monodisperse complex and hierarchical colloidally-stable 2D structures based on PLLA cores using the seeded growth, "living-crystallization-driven self-assembly" method. Specifically, we describe the formation of diamond-shaped platelet micelles and concentric "patchy" block comicelles by using seeds of the charge-terminated homopolymer $PLLA_{24}[PPh_2Me]I$ to initiate the sequential growth of either additional $PLLA_{24}[PPh_2Me]I$ or a crystallizable blend of the latter with the block copolymer $PLLA_{42}$-*b*-$P2VP_{240}$, respectively. The epitaxial nature of the growth processes used for the creation of the 2D block comicelles was confirmed by selected area electron diffraction analysis. Crosslinking of the P2VP corona of the peripheral block in the 2D block comicelles using Pt nanoparticles followed by dissolution of the interior region in good solvent for PLLA led to the formation of novel, hollow diamond-shaped assemblies. We also demonstrate that, in contrast to the aforementioned results, seeded growth of the unsymmetrical PLLA BCPs $PLLA_{42}$-*b*-$P2VP_{240}$ or $PLLA_{20}$-*b*-$PAGE_{80}$ alone from 2D platelets leads to the formation of diamond-fiber hybrid structures.

1. INTRODUCTION

Two-dimensional (2D) planar structures have received extensive recent attention due to their unique properties that originate from their ultrathin and flat morphology.[1] Representative examples include graphene,[2] transition metal dichalcogenide nanosheets,[3] boron nitride,[4] and clay nanoplatelets,[5] which have found applications in electronics, photonics, spintronics, and composite reinforcement. Such materials are generally prepared from bulk layered materials through a "top-down" approach. In contrast, the use of "bottom up" routes to discrete 2D nanostructures are much less explored.[1c, 6-7]

The self-assembly of block copolymers (BCPs) is, in principle a potential route to 2D materials. However, although amorphous block copolymers have been extensively investigated and yield a wide range of micellar nanostructures including spheres, cylindrical or worm-like micelles, and kinetically-trapped morphologies of remarkable complexity, the formation of 2D lamellar platelets is relatively rare.[8] Generally, bilayer structures with flexible cores tend to undergo spontaneous closure to form vesicles. Self-assembly of crystalline homopolymers and BCPs, on the other hand, has recently emerged as a promising route to generate analogous functional 2D materials due to their relative structural rigidity.[9-12] Crystalline homopolymers generally form thin lamellae which are not colloidally stable due to the absence of solvophilic substituents. However, it has been demonstrated that the use of thiol-terminated crystalline homopolymers poly(ethylene oxide) (PEO) and polycaprolactone (PCL) allows peripheral nanoparticle patterning on 2D platelets.[10] Fabrication of alternate rings of a homopolymer and BCP has also been reported, and fluorescent nanosheets have been recently described for π-conjugated homopolymers.[11] In addition, colloidally stable 2D platelets are commonly formed from crystallizable BCPs with short complementary corona-forming block,[11,12] whereas 1D cylindrical micelles are usually favored for BCPs with long corona-forming blocks due to the strong corona-corona repulsions which promote curvature of the core-corona interface.[13]

Precise control of nanoparticle dimensions and their spatially-defined chemistry, together with access to uniform samples, are highly desirable in order to tailor their material properties. The use of crystallization-driven, seeded growth strategies provides a recently established route for the preparation of near monodisperse fiber-like micelles and segmented 1D assemblies of controlled length from BCPs with a crystallizable core-forming block. This has been extensively developed for polyferrocenylsilane (PFS) BCPs[14] over the past decade where sonication of polydisperse fiber-like micelles leads to small seeds which are active to further growth on addition of dissolved BCP (unimer) in a process termed living crystallization-driven self-assembly (CDSA).[15] Similar approaches have been demonstrated for the preparation of analogous 1D mate-

rials with crystallizable organic cores based on polyethylene,[13a-b] π-conjugated polymers,[16] planar, π-stacking molecules,[17] and other self-assembling molecular species.[18] Furthermore, the utility of the living CDSA strategy has been expanded to create uniform 2D structures with well-controlled dimensions.[12f, 19-20] For example, nanosheets formed by the crystallization of precursors containing hyperbranched poly(ether amine) capped with a polyhedral oligomeric silsesquioxane can be fragmented into seeds by sonication, and that these seeds can be used to control the growth of 2D platelets on subsequent precursor addition.[12f] We have demonstrated that precisely defined 2D lenticular and rectangular platelet micelles can be prepared by seeded growth of PFS BCPs and homopolymer/BCP blends, respectively.[19-21] Very recently, we reported a simplified approach to the preparation of uniform, colloidally stable 2D platelets using PFS homopolymers with charged phosphonium cations as termini (e.g. $PFS_{20}[PPh_2Me]I$) in combination with seeded growth.[22] In this case the presence of the charged termini hinders platelet stacking as a result of electrostatic repulsion and provides colloidal stability.

In this report we focus on the extension of seeded growth, living CDSA processes to fabrication of well-controlled and unprecedented hierarchical 2D structures based on crystalline poly(L-lactide) (PLLA). PLLA is a crystallizable polymer of major interest for a variety of applications including in nanomedicine as a consequence of its non-toxicity, biocompatibility and biodegradability.[23] Early work on the self-assembly of PLLA BCPs demonstrated the formation of spheres, cylinders and platelets, often as mixed morphologies.[11b,24] More recently, Dove, O'Reilly and coworkers have exploited the core-crystallization of PLLA BCPs to fabricate a range of well-defined 1D cylindrical micelles.[25] For example, low dispersity cylindrical micelles with lengths up to *ca.* 250 nm were prepared by growth in aqueous media at 65°C, above the glass transition temperature of the PLLA block (55-60 °C). The ability to vary the length of cylindrical micelles based on PLLA BCPs was also demonstrated by varying the composition of the BCPs and solvent.[25] These workers also reported that a 1:1 mixture of cylindrical micelles separately formed by PLLA-*b*-PAA and PDLA-*b*-PAA (PDLA = poly(D-lactide), PAA = poly(acrylic acid)) evolve into spherical micelles with a stereocomplexed PLLA/PDLA core when heated at 65°C.[26]

In contrast to the substantial recent progress with 1D PLLA-based materials, nanoscale 2D platelet structures derived from PLLA BCPs are considerably less explored. Cheng and coworkers reported the growth of single crystalline PLLA from single crystals of PLLA-PS (PS = polystyrene) BCP.[11b] In recent work, Xie and Wang and coworkers reported the formation of 2D platelets of PLLA-PEG (PEG = poly(ethylene glycol)) via a morphological transition from spheres.[27] In addition, Dove, O'Reilly and coworkers have further examined the factors that influence the formation of 1D and 2D morphologies by PLLA BCPs and have described the formation of well-defined platelet micelles and also routes to hierarchical assemblies from 1D and 2D components by the use of BCP blends. [28]

As part of our recent report on the formation of 2D materials by the seeded growth of PFS homopolymers with charged termini, we also described the extension of this approach to charge-terminated PLLA homopolymers $PLLA_m[PPh_2Me]I$ (m = 24 and 34), to obtain monodisperse colloidally-stable diamond-shaped 2D platelets of controlled area.[22] Such a morphology is well-established for PLLA single crystals.[11b,12k,28] In addition, we reported preliminary details of the formation of segmented 2D platelets via the sequential addition of further $PLLA_m[PPh_2Me]I$ together with PLLA homopolymer with a terminal fluorescent dye.[22] Herein, we report the fabrication of well-controlled and unprecedented hierarchical PLLA-based structures, including diamond-shaped "patchy" platelet block comicelles, hollow platelet micelles and diamond-fiber hybrid structures by the use of seeded growth and post-assembly processing approaches. The work demonstrates that the use of seeded growth, living CDSA methods represents a powerful approach to not only PFS-based 2D materials, but also to those based on other functional organic polymers.

2. RESULTS AND DISCUSSION

Synthesis and Characterization of PLLA BCPs. To perform the targeted living CDSA experiments we prepared several PLLA-based materials as building blocks. The charge-terminated $PLLA_{24}[PPh_2Me]I$ homopolymer (the subscript refers to the number average degree of polymerization, Figure 1) possessing a phosphonium end group was prepared by ring-opening polymerization (ROP) of L-lactide monomer initiated with a phosphine-substituted alcohol followed by quaternization with MeI.[22] Two PLLA BCPs, $PLLA_{42}$-*b*-$P2VP_{240}$ (P2VP = poly(2-vinylpyridine)) and $PLLA_{20}$-*b*-$PAGE_{80}$ (PAGE = poly(allyl glycidyl ether)) were also prepared (Figure 1). Synthesis of $PLLA_{42}$-*b*-$P2VP_{240}$ BCP was carried out by combining reverse-addition fragmentation chain transfer (RAFT) polymerization and Ring-Opening Polymerization (ROP) techniques.[25] A PLLA macroinitiator suitable for RAFT was prepared by ROP and this was then used to polymerize 2VP. This two-step synthesis produced $PLLA_{42}$-*b*-$P2VP_{240}$ in a yield 70 % and PDI of 1.21. The detailed procedure for $PLLA_{42}$-*b*-$P2VP_{240}$ is summarized in Scheme S1 in the supporting information. $PLLA_{20}$-*b*-$PAGE_{80}$, on the other hand, was prepared according to a reported procedure,[29] by one-step ROP of L-lactide by $PAGE_{80}$-OH as macroinitiator also in *ca.* 70% yield, with a low polydispersity index (PDI) of 1.05. Detailed characterization of the BCPs $PLLA_{42}$-*b*-$P2VP_{240}$ and $PLLA_{20}$-*b*-$PAGE_{80}$ are described in the supporting information and in Figure S1-S6.

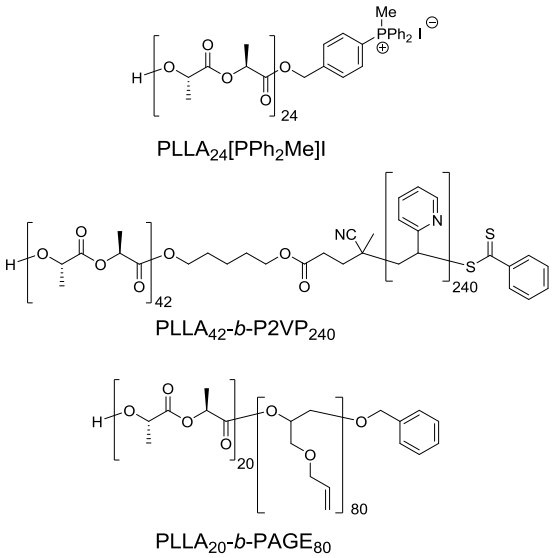

Figure 1. Chemical structures of $PLLA_{24}[PPh_2Me]I$, $PLLA_{42}$-*b*-$P2VP_{240}$ and $PLLA_{20}$-*b*-$PAGE_{80}$.

Diamond-Shaped Platelet Micelles and "Patchy" Block Comicelles Prepared by Seeded Growth. In addition to the self-assembly studies for amorphous blends of BCP and homopolymer,[21] similar experiments have been performed for crystallizable analogues in the absence of seeds. For example, Eisenberg and van de Ven and coworkers previously reported the preparation for non-uniform 2D assemblies based on crystalline poly(ε-caprolactone) (PCL) cores by blending PCL-*b*-PEO BCP and PCL homopolymer.[30a-b] Analogous polydisperse platelets have been reported for crystallizable blends of PFS BCPs and homopolymer.[30c] Recently, we have shown that the seeded growth of crystallizable blends of BCP and homopolymer, or of a crystallizable charge-terminated homopolymer, allows the formation of uniform 2D platelet micelles and block comicelles with controlled dimensions.[20,22] In this work we explored the use of the latter strategies for the fabrication of well-controlled, complex, and hierarchical PLLA-based assemblies.

In our initial experiments we examined the growth of the blend of $PLLA_{42}$-*b*-$P2VP_{240}$ and the charge-terminated homopolymer $PLLA_{24}[PPh_2Me]I$ from quasi-1D seeds of $PLLA_{24}[PPh_2Me]I$ (L_n = 200 nm, L_w/L_n = 1.09, where L_w is the weight-average length and L_n is the number-average length). The seeds were prepared by sonication of 2D platelets of $PLLA_{24}[PPh_2Me]I$ (0.1 mg/mL) in iPrOH/$CHCl_3$ (10:1), according to our previous report.[22] Because both the phosphonium moiety and the P2VP block are solvated in polar solvents such as iPrOH, in which the PLLA block is insoluble, iPrOH was chosen as a suitable selective solvent for the self-assembly experiments.

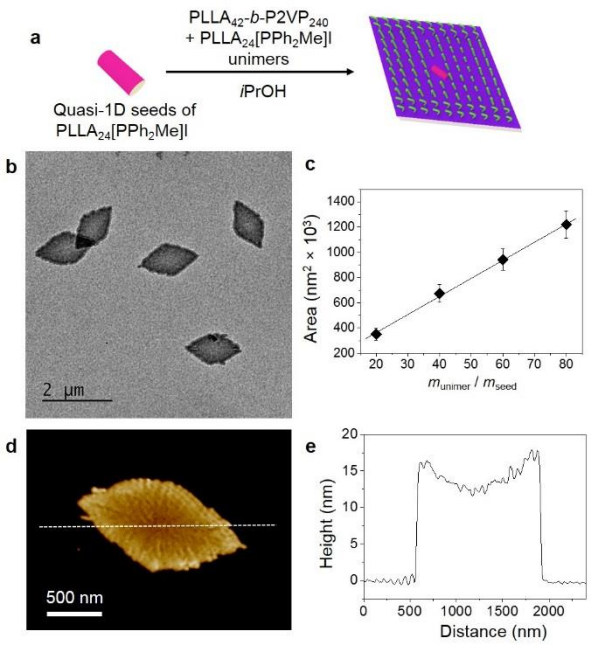

Figure 2. (a) Schematic representation for the formation of 2D diamond-shaped platelet micelle through seeded growth of $PLLA_{42}$-*b*-$P2VP_{240}$/$PLLA_{24}[PPh_2Me]I$ (1:1, mass ratio) blend unimer from quasi-1D seeds of $PLLA_{24}[PPh_2Me]I$ in iPrOH; (b) its corresponding TEM image with unimer to seed mass ratio (m_{unimer}/m_{seed}) of 80, the sample for TEM was not stained; (c) Linear dependence of micelle area on the m_{unimer}/m_{seed}. Error bars, standard deviation of measured areas; (d) AFM image with m_{unimer}/m_{seed} of 80; (e) the height profile of platelet comicelles.

As shown in Figure 2, addition of a solution of molecularly dissolved $PLLA_{42}$-*b*-$P2VP_{240}$/$PLLA_{24}[PPh_2Me]I$ blend (1:1, mass ratio) unimers in $CHCl_3$ to quasi-1D small seed of $PLLA_{24}[PPh_2Me]I$ in iPrOH led to uniform diamond-shaped platelet micelles, demonstrating the control implicit in this approach. The area of the platelets was found to be linearly dependent on the unimer-to-seed mass ratio (m_{unimer}/m_{seed}) and the area dispersity was very low (A_w/A_n = 1.02, where A_w is the weight-average area and A_n is the number-average area). The contour areas for the platelets are summarized in Figure S7 and Table S1. The heights of the platelet by atomic force microscopy (AFM) were found to be *ca.* 15 nm on average, and the height of the edge (17 nm) was higher than the center (13 nm), probably due to the uneven distribution of PLLA homopolymer and BCP on the surface of the formed platelet because of their likely difference in epitaxial growth rate (Figure 2d-e).

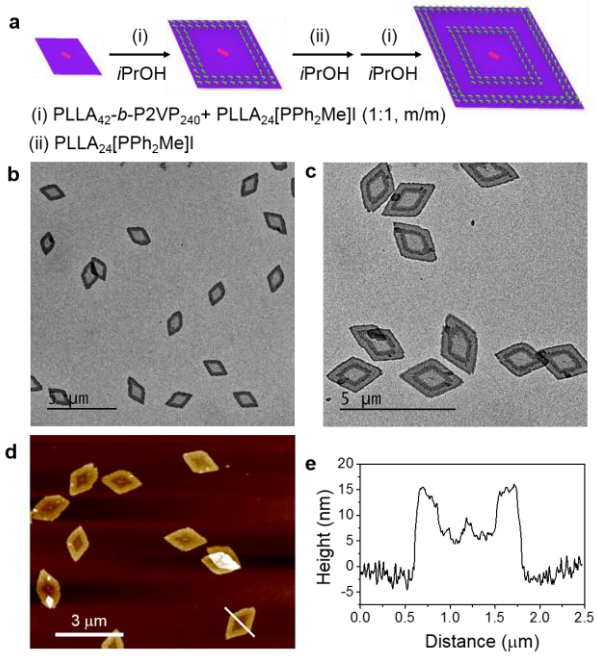

Figure 3. (a) Schematic representation of the formation of diamond-shaped "patchy" platelet block comicelles through seeded growth. TEM images of (b) diblock and (c) tetra-block platelet comicelles. The samples for TEM were not stained. (d) AFM image and (e) the height profile of diblock platelet comicelle.

Encouraged by these results, we attempted to fabricate "patchy" diamond-shaped platelet block comicelles. Firstly, large diamond platelets (A_n = 394,770 nm^2, A_w/A_n = 1.04) were prepared by seeded growth of $PLLA_{24}[PPh_2Me]I$ unimers in $CHCl_3$ from quasi-1D small seed of $PLLA_{24}[PPh_2Me]I$ in iPrOH. Then, addition of the unimeric polymer blend $PLLA_{42}$-*b*-$P2VP_{240}$/$PLLA_{24}[PPh_2Me]I$ in $CHCl_3$ to the diamond shaped platelets derived from $PLLA_{24}[PPh_2Me]I$ in iPrOH yielded segmented block platelet comicelles, as shown Figure 3 and S8. Different blend ratios of $PLLA_{42}$-*b*-$P2VP_{240}$/$PLLA_{24}[PPh_2Me]I$ (4:1, 1:1 and 1:4, based on mass ratio) were all found to form platelet structures (Figure S8). A 1:1 mass ratio of BCP and homopolymer was found to give best control of the formation of "patchy" diamond-shaped platelet, which will be used throughout. The peripheral block was clearly observed as darker region in TEM image, due to the higher electron density of the P2VP corona. AFM images showed a clear height difference between the two spatially distinct regions, with the second block formed by the $PLLA_{42}$-*b*-$P2VP_{240}$/$PLLA_{24}[PPh_2Me]I$ polymer blend (1:1, mass ratio) higher than the first block composed of $PLLA_{24}[PPh_2Me]I$ (18 nm v.s. 9 nm, respectively). The higher peripheral region is a consequence of the presence of the long P2VP block. Further sequential alternating addition of unimers $PLLA_{24}[PPh_2Me]I$ and a $PLLA_{42}$-*b*-$P2VP_{240}$/$PLLA_{24}[PPh_2Me]I$ blend (1:1, mass ratio), resulted in concentric segmented platelet comicelles with four distinct regions of excellent contrast were formed based on TEM (Figure 3c). These experiments demonstrated the formation of 2D platelets by the seeded growth of a crystallizable blend of BCP and homopolymer is not limited to PFS-based polymers but also applicable for PLLA-based polymers.

In order to confirm that the growth of the platelets was driven by epitaxial growth, selected-area electron diffraction (SAED) analysis of platelet micelle and block comicelle was carried out. As shown in Figure 4, both the platelet micelle precursor (Figure 4a,b) and block comicelle (Figure 4c-e) possess identical ED patterns with three pairs of diffraction spots, confirming that PLLA core in these two cases consists of a single crystalline layer and the growth of 2D block comicelle is driven by epitaxial crystallization. These SAED patterns are assigned to be the [001] zone pattern of the orthorhombic (α) form of PLLA. These 2D platelets are bound by four (110) planes. ED analysis showed that the observed pattern contains four (110) planes with the d-spacing of 0.537 nm and two (200) planes having the d-spacing of 0.543 nm, which is consistent to the case of PLLA solution-grown crystals.[24g] A similar platelet morphology and SAED pattern were also observed for lamellar single crystals of PLLA-*b*-PS (19.9K-9.2K) by Cheng and coworkers.[11b]

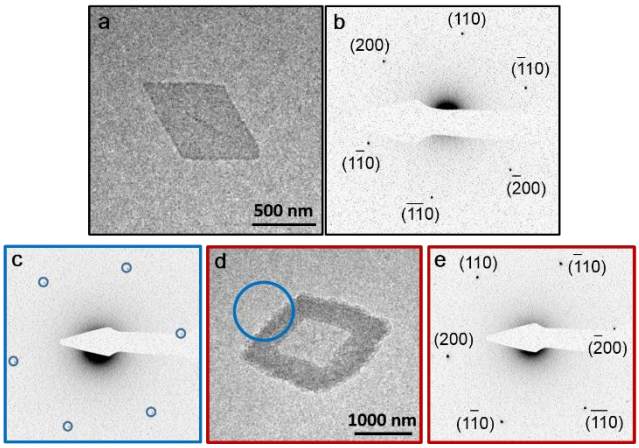

Figure 4. TEM images and selected area electron diffraction (SAED) patterns for platelet micelles (a,b) and comicelles (c-e). The black square in (a) and red square and blue circle in (d) represent the selected areas for the electron diffraction in (b), (c) and (e), in which the surrounding lines are labeled with the same colors. A relatively large area was used in (d) to maximize data quality. No diffraction from the surrounding carbon film was detected. The samples analysed by TEM were not stained.

Hollow Diamond-Shaped Platelet Micelles. Crosslinking of the core or corona/shell of micelles is a well-established method for the generation of micelles with improved stability.[31] The resulting micelles are resistant to dissolution and maintain their structure in good solvents. For instance, the P2VP coronas of the branched cylindrical micelles could be cross-linked by Karstedt's catalyst through the formation of small Pt nanoparticles with Pt coordination to the pyridyl groups on P2VP.[32] Although cross-linking has been widely used in a wide range of nanomaterials, its application in the fabrication of hollow platelet structures is very rare. This is a consequence of the limited methods for creating multicompartmental platelets. We have recently demonstrated that uniform hollow rectangular structures based on PFS systems could be prepared by controlling the cross-linking in a spatial-

ly selective manner, followed by dissolution of uncrosslinked regions in a good solvent for the core.[20, 31b] However, analogous hollow structures derived from organic polymers have not been reported.

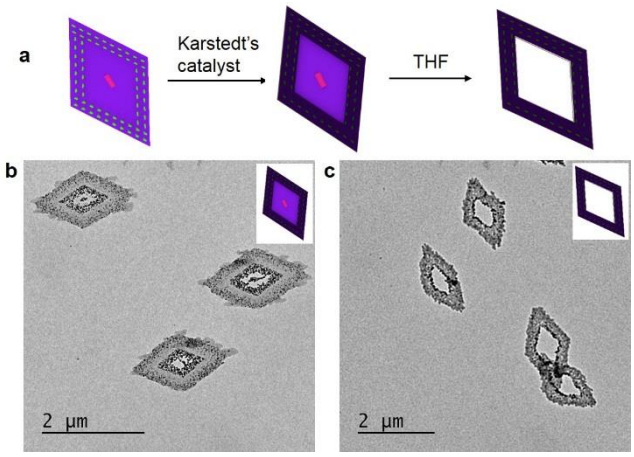

Figure 5. (a) Schematic representation for the formation of cross-linked platelet block comicelle and hollow micelles, and (b,c) their corresponding TEM images. The samples analysed by TEM were not stained.

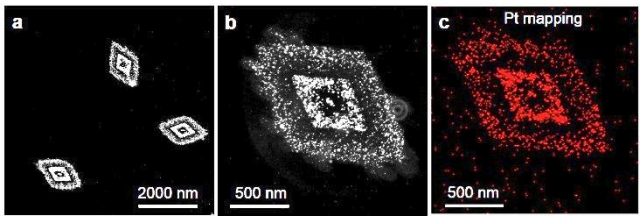

Figure 6. (a,b) Dark-field TEM image of cross-linked platelet comicelle. The central region is derived from $PLLA_{24}[PPh_2Me]I$ and the peripheral block is derived from $PLLA_{42}$-*b*-$P2VP_{240}$/ $PLLA_{24}[PPh_2Me]I$ (1:1, mass ratio). (c) STEM-EDX Pt element (red) mapping.

In order to fabricate hollow diamond-shaped platelets, we selected a concentric diamond-shaped platelet block comicelles, with the central block derived from $PLLA_{24}[PPh_2Me]I$ and peripheral block derived from with $PLLA_{42}$-*b*-$P2VP_{240}$/ $PLLA_{24}[PPh_2Me]I$ blend (1:1, m/m) (Figure 3b and d). We found that Karstedt's catalyst can effectively crosslink the peripheral block consisting of $PLLA_{42}$-*b*-$P2VP_{240}$/ $PLLA_{24}[PPh_2Me]I$, by the formation of Pt nanoparticles (Figure 5 and 6, S9). By using scanning transmission electron microscopy energy-dispersive X-ray (STEM-EDX) in elemental mapping mode, the distribution of elemental Pt was directly revealed on the platelets (Figure 6c); their location matched well with the nanoparticle area, conforming that nanoparticles are mainly composed of Pt (Figure 6). A high-resolution TEM image of the Pt nanoparticles showed that they possess a diameter of 9-10 nm and also that they lead to crystalline patterns (Figure S9). The height of the cross-linked regions of the platelet was measured to be 5-10 nm higher than that of non-crosslinked platelet (Figure S10a). By removing the iPrOH and dispersing the cross-linked structure in THF, a diamond-shaped hollow structure was produced (Figure 5c and S10). The presence of hollow interior was confirmed by the AFM, with the central height near to zero. In contrast to the use of Karstedt's catalyst alone, the combination of Karstedts catalyst and 1,1,3,3-tetramethyldisiloxane (TMDS), which leads to crosslinking via hydrosilylation,[33] was found to lead to severe aggregation (Figure S11).

Diamond-Fiber Hybrid Structures. We have demonstrated that seeded growth of either $PLLA_{24}[PPh_2Me]I$ homopolymer or a $PLLA_{42}$-*b*-$P2VP_{240}$/$PLLA_{24}[PPh_2Me]I$ blend from quasi-1D seeds or preformed 2D platelets leads to controlled formation of diamond-shaped platelets. Strikingly, addition of solely $PLLA_{42}$-*b*-$P2VP_{240}$ BCP in $CHCl_3$ to the $PLLA_{24}[PPh_2Me]I$ diamond platelet (A_n = 394,770 nm^2, A_w/A_n = 1.04) in iPrOH led to diamond-fiber hybrid structures (Figure 7b). The added $PLLA_{42}$-*b*-$P2VP_{240}$ BCP grew as fibers from the four edges of all the platelets. Similar hierarchical structures (Figure 7e) were also formed by addition of $PLLA_{20}$-*b*-$PAGE_{80}$ unimer in THF to the $PLLA_{24}[PPh_2Me]I$ platelets in iPrOH, indicating that the formation of diamond-fiber hybrid structures is adaptable to other PLLA BCPs with a different corona. However, aggregation between the hybrid structures was observed by TEM due to the growth of $PLLA_{20}$-*b*-$PAGE_{80}$ fibers which tend to associate through the PAGE coronas. In addition, the length of the $PLLA_{20}$-*b*-$PAGE_{80}$ fibers was found to be linearly dependent on the unimer-to-seed mass ratio (m_{unimer}/m_{seed}), consistent with a living CDSA process (Figure S12).

Moreover, diamond-fiber (block)-like structures with fibers containing spatially segregated coronal chemistries could be formed by further addition of different BCPs to the hybrid diamond-fiber-like structures (F@D). Thus, addition of $PLLA_{20}$-*b*-$PAGE_{80}$ unimer to diamond-fiber-hybrid structure F{$PLLA_{42}$-*b*-$P2VP_{240}$}@D, was found to afford the anticipated diamond-fiber (block)-like structures F{$PLLA_{20}$-*b*-$PAGE_{80}$}-*b*-F{$PLLA_{42}$-*b*-$P2VP_{240}$}@D (Figure 7c). Similarly, addition of $PLLA_{42}$-*b*-$P2VP_{240}$ unimer to diamond-fiber-like structure F{$PLLA_{20}$-*b*-$PAGE_{80}$}@D, led to the formation of diamond-fiber (block)-like structures F{$PLLA_{42}$-*b*-$P2VP_{240}$}-*b*-F{$PLLA_{20}$-*b*-$PAGE_{80}$}@D (Figure 7f). In the two diamond-fiber (block)-like structures mentioned above (Figure 7c and 7f), two blocks of fibers be differentiated by the TEM due to their different contrast, and the second BCPs grows epitaxially at the end of the first block fibers. It was also noteworthy that severe aggregation was observed by TEM for the two diamond-fiber (block)-like structures due to the presence of the PAGE corona (Figure S13). In our previous report, scarf-like micelles with cylindrical fibers selectively grown from the long-axis platelet end were formed by addition of PFS BCPs to rectangular platelets derived from PFS polymers.[34] The selective nature of the epitaxial growth in the PFS system was attributed to the preferred direction of crystal growth along the long axis (b axis, [010] direction).[35] In contrast, the crystal growth of the diamond-shaped PLLA platelet is isotropic along all four [110] directions, therefore preferring the growth of fibers at four edges with similar growth rates.

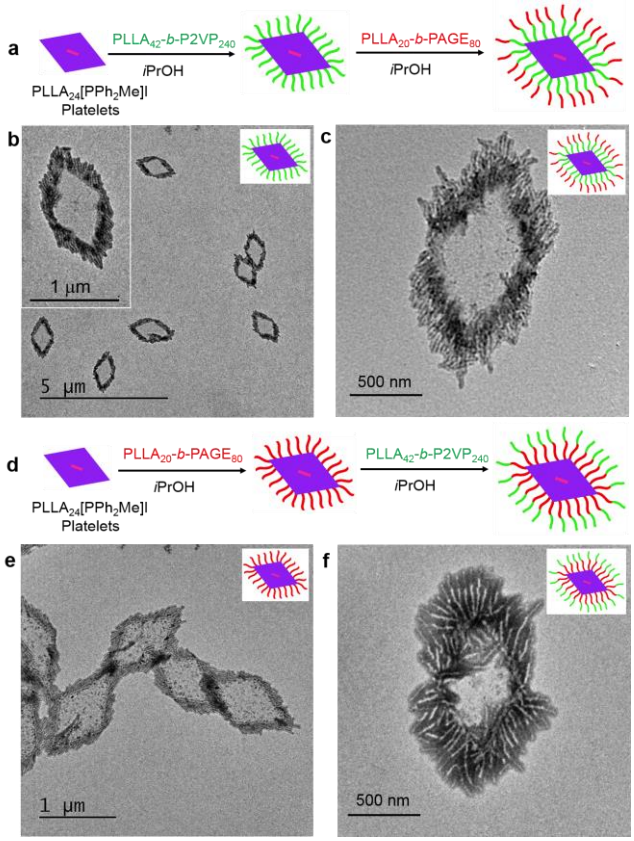

Figure 7. Schematic representation (a, d) and TEM images (b, c, e, f) of diamond-fiber hybrid structures F{PLLA$_{42}$-*b*-P2VP$_{240}$}@D (b), F{PLLA$_{20}$-*b*-PAGE$_{80}$}@D (e), and diamond-fiber(block)-like structures, F{PLLA$_{20}$-*b*-PAGE$_{80}$}-*b*-F{PLLA$_{42}$-*b*-P2VP$_{240}$}@D (c), F{PLLA$_{42}$-*b*-P2VP$_{240}$}-*b*-F{PLLA$_{20}$-*b*-PAGE$_{80}$}@D (f). F = fiber, D = diamond. In (c) and (f) severe aggregation was also observed due to coronal association of the PLLA$_{20}$-*b*-PAGE$_{80}$ fibers (see Figure S13). A single dispersed micelle is shown for clarity. The samples for TEM were not stained.

Patterning of diamond-shaped pletelets with SiO_2 nanoparticles (NPs): Electrostatic interactions have been used for the controlled patterning of negatively SiO_2 nanoparticles on PFS-derived rectangular platelets with positive surfaces in a controlled manner.[22] It is expected that a choice of different shape of 2D platelet would tune the patterning mode of SiO_2 NPs with different shape, which might be important for tuning the property of materials. Here, we selected two different sizes of diamond-shaped platelets (A_n = 394,770 nm^2, A_w/A_n = 1.04; A_n = 1985,400 nm^2, A_w/A_n = 1.03) derived from PLLA$_{24}$[PPh$_2$Me]I as templates to investigate the patterning mode of SiO_2 NPs.

A layer-by-layer approach was applied for the SiO_2 NPs patterning, similar to our previous reported procedure.[22] Platelet micelles derived from PLLA$_{24}$[PPh$_2$Me]I were drop-cast and dried on carbon-coated TEM grids in air. These grids were then immersed in the ethanol solution of SiO_2 NPs (diameter = 55 nm) for 30 min. Then iPrOH was used to remove the free SiO_2 NPs on the grids after the incubation. Figure S14 shows the pattern of SiO_2 NPs loading on the PLLA$_{24}$[PPh$_2$Me]I platelets with two different sizes (S14a: small size platelets; S14b: large size platelet). All of the plates were loaded with SiO_2 NPs, and no free platelets or SiO_2 NPs were found on the TEM grid, indicating the specific loading due to the mutual electrostatic interaction. The SiO_2 NP loading density on the platelet edge was found to be slightly higher than that in the center, perhaps as a consequence of the lower steric encumbrance at the platelet boundary.

3. SUMMARY

Soft matter-based nanoparticles are attractive for a broad range of applications. 2D assemblies are of particular current interest but the control of dimensions and spatial functionality represents a key challenge. In this paper we have successfully demonstrated the formation of a range of novel PLLA-based hierarchical platelet structures, such as diamond-shaped "patchy" platelet block comicelles, hollow platelets and diamond-fiber hybrid structures prepared by seeded growth of either PLLA homoplymer and/or BCPs. The key to the preparation of these structures is the seeded growth living CDSA approach that allows precise control of the assembly process. Thus, seeded growth of a PLLA$_{42}$-*b*-P2VP$_{240}$/PLLA$_{24}$[PPh$_2$Me]I polymer blend from both small quasi-1D seeds and large 2D diamond-shaped platelet micelles derived from PLLA$_{24}$[PPh$_2$Me]I leads to the formation of well-defined diamond-shaped platelets and 'patchy' platelet block comicelles, respectively. This 2D living process is driven by an epitaxial growth mechanism, which was also confirmed by electron diffraction. Uniform hollow diamond-shaped structures could be produced by selectively cross-linking the peripheral block derived from PLLA$_{42}$-*b*-P2VP$_{240}$/ PLLA$_{24}$[PPh$_2$Me]I of diamond-shaped platelet block comicelles with a central block derived from PLLA$_{24}$[PPh$_2$Me]I, followed by dissolution of the central block in a good solvent. On the other hand, addition solely of a cylinder-forming BCP led to the growth of fibers from four edges of the diamond-shaped platelet. Patterning of SiO_2 NPs on the diamond-shaped platelets has also been demonstrated.

Previous work has illustrated the promise of the living CDSA approach to 1D and 2D soft matter-based nanoparticles. However, the vast majority of the work to date has focused on PFS homopolymers and BCPs. In this paper we have shown that this approach represents a powerful route to uniform, complex and hierarchical assemblies based on PLLA, a biodegradable organic polymer of considerable current interest for the development of release vehicles for pharmaceutical and other applications. Further studies directed towards these end-uses are currently underway. For example, we are currently studying the introduction of more hydrophilic charged termini to PLLA in order to permit self-assembly in aqueous media.

ASSOCIATED CONTENT

Supporting Information

Experimental procedures and additional data. This material is available free of charge via the Internet at http://pubs.acs.org.

AUTHOR INFORMATION

Corresponding Author

*To whom correspondence should be addressed:
ian.manners@bristol.ac.uk

ORCID

Xiaoming He: 0000-0003-2596-7042
Yunxiang He: 0000-0001-5275-2691
Ming-Siao Hsiao: 0000-0001-9319-653x
Mitchell A. Winnik: 0000-0002-2673-2141
Ian Manners: 0000-0002-3794-967x

Notes

The anthors declare no competing financial interest.

ACKNOWLEDGMENT

X.M.H. is grateful to the European Union (EU) for a Marie Curie Postdoctoral Fellowship. Y. H. and S. P. thank the Bristol Chemical Synthesis Centre for Doctoral Training and Bristol Centre for Functional Nanomaterials, founded by the Engineering and Physical Sciences Research Council (EPSRC), for a PhD studentship. PeakForce atomic force microscopy was carried out in the Chemical Imaging Facility, University of Bristol, with equipment funded by EPSRC. We thank Mr. Jonathan Jones for the help with the STEM-EDX measurement.

REFERENCES

(1) a) Zhang, X.; Xie, Y. *Chem. Soc. Rev.* **2013**, *42*, 8187; b) Zhuang, X.; Mai, Y.; Wu, D.; Zhang, F.; Feng, X. *Adv. Mater.* **2015**, *27*, 403; c) Boott, C. E.; Nazemi, A.; Manners, I. *Angew. Chem. Int. Ed.* **2015**, *54*, 13876.

(2) a) Geim, A. K.; Novoselov, K. S. *Nat. Mater.* **2007**, *6*, 183; b) Lin, Y.-M.; Dimitrakopoulos, C.; Jenkins, K. A.; Farmer, D. B.; Chiu, H.-Y.; Grill, A.; Avouris, P. *Science* **2010**, *327*, 662.

(3) Splendiani, A.; Sun, L.; Zhang, Y.; Li, T.; Kim, J.; Chim, C.-Y.; Galli, G.; Wang, F. *Nano Lett.* **2010**, *10*, 1271.

(4) a) Golberg, D.; Bando, Y.; Huang, Y.; Terao, T.; Mitome, M.; Tang, C.; Zhi, C. *ACS Nano* **2010**, *4*, 2979; b) Gibb, A. L.; Alem, N.; Chen, J.-H.; Erickson, K. J.; Ciston, J.; Gautam, A.; Linck, M.; Zettl, A. *J. Am. Chem. Soc.* **2013**, *135*, 6758.

(5) a) Ras, R. H. A.; Umemura, Y.; Johnston, C. T.; Yamagishi, A.; Schoonheydt, R. A. *Phys. Chem. Chem. Phys.* **2007**, *9*, 918; b) Takagi, S.; Shimada, T.; Ishida, Y.; Fujimura, T.; Masui, D.; Tachibana, H.; Eguchi, M.; Inoue, H. *Langmuir* **2013**, *29*, 2108.

(6) Sakamoto, R.; Hoshiko, K.; Liu, Q.; Yagi, T.; Nagayama, T.; Kusaka, S.; Tsuchiya, M.; Kitagawa, Y.; Wong, W.-Y.; Nishihara, H. *Nat. Commun.* **2015**, *6*, 6713.

(7) Schlüter, A. D.; Payamyar, P.; Öttinger, H. C. *Macromol. Rapid Commun.* **2016**, *37*, 1638.

(8) a) Mai, Y.; Eisenberg, A. *Chem. Soc. Rev.* **2012**, *41*, 5969; b) Dupont, J.; Liu, G. *Soft Matter* **2010**, *6*, 3654; c) Pochan, D. J.; Chen, Z.; Cui, H.; Hales, K.; Qi, K.; Wooley, K. L. *Science* **2004**, *306*, 94; d) Groschel, A. H.; Walther, A.; Lobling, T. I.; Schacher, F. H.; Schmalz, H.; Muller, A. H. E. *Nature* **2013**, *503*, 247; e) Jang, S. G.; Audus, D. J.; Klinger, D.; Krogstad, D. V.; Kim, B. J.; Cameron, A.; Kim, S.-W.; Delaney, K. T.; Hur, S.-M.; Killops, K. L.; Fredrickson, G. H.; Kramer, E. J.; Hawker, C. J. *J. Am. Chem. Soc.* **2013**, *135*, 6649; f) Hayward, R. C.; Pochan, D. J. *Macromolecules* **2010**, *43*, 3577.

(9) a) Keller, A. *Polymer* **1962**, *3*, 393; b) Lotz, B.; Kovacs, A. J.; Bassett, G. A.; Keller, A. *Kolloid Z. Z. Polym.* **1966**, *209*, 115.

(10) a) Li, B.; Li, C. Y. *J. Am. Chem. Soc.* **2007**, *129*, 12; b) Dong, B.; Zhou, T.; Zhang, H.; Li, C. Y. *ACS Nano* **2013**, *7*, 5192.

(11) a) Chen, W. Y.; Li, C. Y.; Zheng, J. X.; Huang, P.; Zhu, L.; Ge, Q.; Quirk, R. P.; Lotz, B.; Deng, L.; Wu, C.; Thomas, E. L.; Cheng, S. Z. D. *Macromolecules* **2004**, *37*, 5292; b) Zheng, J. X.; Xiong, H.; Chen, W. Y.; Lee, K.; Van Horn, R. M.; Quirk, R. P.; Lotz, B.; Thomas, E. L.; Shi, A.-C.; Cheng, S. Z. D. *Macromolecules* **2006**, *39*, 641; c) Yang, S.; Shin, S.; Choi, I.; Lee, J.; Choi, T.-L. *J. Am. Chem. Soc.* **2017**, *139*, 3082.

(12) a) Cao, L.; Manners, I.; Winnik, M. A. *Macromolecules* **2002**, *35*, 8258; b) Mohd Yusoff, S. F.; Hsiao, M.-S.; Schacher, F. H.; Winnik, M. A.; Manners, I. *Macromolecules* **2012**, *45*, 3883; c) Su, M.; Huang, H.; Ma, X.; Wang, Q.; Su, Z. *Macromol. Rapid Commun.* **2013**, *34*, 1067; d) Wang, J.; Zhu, W.; Peng, B.; Chen, Y. *Polymer* **2013**, *54*, 6760; e) Tong, Z.; Li, Y.; Xu, H.; Chen, H.; Yu, W.; Zhuo, W.; Zhang, R.; Jiang, G. *ACS Macro Lett.* **2016**, *5*, 867; f) Yu, B.; Jiang, X.; Yin, J. *Macromolecules* **2014**, *47*, 4761; g) Zhu, W.; Peng, B.; Wang, J.; Zhang, K.; Liu, L.; Chen, Y. *Macromol. Biosci.* **2014**, *14*, 1764; h) Wu, J.; Weng, L.-T.; Qin, W.; Liang, G.; Tang, B. Z. *ACS Macro Lett.* **2015**, *4*, 593; i) Tong, Z.; Li, Y.; Xu, H.; Chen, H.; Yu, W.; Zhuo, W.; Zhang, R.; Jiang, G. *ACS Macro Lett.* **2016**, *5*, 867; j) Fan, B.; Wang, R.-Y.; Wang, X.-Y.; Xu, J.-T.; Du, B.-Y.; Fan, Z.-Q. *Macromolecules* **2017**, *50*, 2006; k) Chiang, Y.-W.; Hu, Y.-Y.; Li, J.-N.; Huang, S.-H.; Kuo, S.-W. *Macromolecules* **2015**, *48*, 8526.

(13) a) Schmelz, J.; Karg, M.; Hellweg, T.; Schmalz, H. *ACS Nano* **2011**, *5*, 9523; b) Schmelz, J.; Schedl, A. E.; Steinlein, C.; Manners, I.; Schmalz, H. *J. Am. Chem. Soc.* **2012**, *134*, 14217; c) Mihut, A. M.; Drechsler, M.; Möller, M.; Ballauff, M. *Macromol. Rapid Commun.* **2010**, *31*, 449; d) Du, Z.-X.; Xu, J.-T.; Fan, Z.-Q. *Macromolecules* **2007**, *40*, 7633; e) He, W.-N.; Zhou, B.; Xu, J.-T.; Du, B.-Y.; Fan, Z.-Q. *Macromolecules* **2012**, *45*, 9768; f) Yang, J.-X.; Fan, B.; Li, J.-H.; Xu, J.-T.; Du, B.-Y.; Fan, Z.-Q. *Macromolecules* **2016**, *49*, 367; g) Lazzari, M.; Scalarone, D.; Vazquez-Vazquez, C.; López-Quintela, M. A. *Macromol. Rapid Commun.* **2008**, *29*, 352; h) Massey, J. A.; Temple, K.; Cao, L.; Rharbi, Y.; Raez, J.; Winnik, M. A.; Manners, I. *J. Am. Chem. Soc.* **2000**, *122*, 11577; i) Lee, I.-H.; Amaladass, P.; Yoon, K.-Y.; Shin, S.; Kim, Y.-J.; Kim, I.; Lee, E.; Choi, T.-L. *J. Am. Chem. Soc.* **2013**, *135*, 17695; j) Brubaker, C. E.; Velluto, D.; Demurtas, D.; Phelps, E. A.; Hubbell, J. A. *ACS Nano* **2015**, *9*, 6872; k) Lazzari, M.; López-Quintela, M. A. *Macromol. Rapid Commun.* **2009**, *30*, 1785; l) Gao, Y.; Li, X.; Hong, L.; Liu, G. *Macromolecules* **2012**, *45*, 1321; m) Schöbel, J.; Karg, M.; Rosenbach, D.; Krauss, G.; Greiner, A.; Schmalz, H. *Macromolecules* **2016**, *49*, 2761; n) Lee, C.-U.; Lu, L.; Chen, J.; Garno, J. C.; Zhang, D. *ACS Macro Lett.* **2013**, *2*, 436.

(14) Hailes, R. L. N.; Oliver, A. M.; Gwyther, J.; Whittell, G. R.; Manners, I. *Chem. Soc. Rev.* **2016**, *45*, 5358.

(15) a) Wang, X.; Guerin, G.; Wang, H.; Wang, Y.; Manners, I.; Winnik, M. A. *Science* **2007**, *317*, 644; b) Gilroy, J. B.; Gädt, T.; Whittell, G. R.; Chabanne, L.; Mitchels, J. M.; Richardson, R. M.; Winnik, M. A.; Manners, I. *Nat. Chem.* **2010**, *2*, 566; c) Hudson, Z. M.; Lunn, D. J.; Winnik, M. A.; Manners, I. *Nat. Commun.* **2014**, *5*, 3372; d) Boott, C. E.; Gwyther, J.; Harniman, R. L.; Hayward, D. W.; Manners, I. *Nat. Chem.* **2017**, doi:10.1038/nchem.2721.

(16) a) Gwyther, J.; Gilroy, J. B.; Rupar, P. A.; Lunn, D. J.; Kynaston, E.; Patra, S. K.; Whittell, G. R.; Winnik, M. A.; Manners, I. *Chem. Eur. J.* **2013**, *19*, 9186; b) Qian, J.; Li, X.; Lunn, D. J.; Gwyther, J.; Hudson, Z. M.; Kynaston, E.; Rupar, P. A.; Winnik, M. A.; Manners, I. *J. Am. Chem. Soc.* **2014**, *136*, 4121.

(17) a) Zhang, W.; Jin, W.; Fukushima, T.; Saeki, A.; Seki, S.; Aida, T. *Science* **2011**, *334*, 340; b) Zhang, W.; Jin, W.; Fukushima, T.; Mori, T.; Aida, T. *J. Am. Chem. Soc.* **2015**, *137*, 13792; c) Ma, X.; Zhang, Y.; Zhang, Y.; Liu, Y.; Che, Y.; Zhao, J. *Angew. Chem. Int. Ed.* **2016**, *55*, 9539; d) Ogi, S.; Sugiyasu, K.; Manna, S.; Samitsu, S.; Takeuchi, M. *Nat. Chem.* **2014**, *6*, 188; e) Ogi, S.; Stepanenko, V.; Sugiyasu, K.; Takeuchi, M.; Würthner, F. *J. Am. Chem. Soc.* **2015**, *137*, 3300; f) Fukui, T.; Kawai, S.; Fujinuma, S.; Matsushita, Y.; Yasuda, T.; Sakurai, T.; Seki, S.; Takeuchi, M.; Sugiyasu, K. *Nat. Chem.* **2016**, doi:10.1038/nchem.2684.

(18) a) Pal, A.; Malakoutikhah, M.; Leonetti, G.; Tezcan, M.; Colomb-Delsuc, M.; Nguyen, V. D.; van der Gucht, J.; Otto, S. *Angew. Chem. Int. Ed.* **2015**, *54*, 7852; b) Aliprandi, A.; Mauro, M.; De Cola, L. *Nat. Chem.* **2016**, *8*, 10; c) Robinson, M. E.; Lunn, D. J.; Nazemi, A.; Whittell, G. R.; De Cola, L.; Manners, I. *Chem. Commun.* **2015**, *51*, 15921.

(19) Hudson, Z. M.; Boott, C. E.; Robinson, M. E.; Rupar, P. A.; Winnik, M. A.; Manners, I. *Nat. Chem.* **2014**, *6*, 893.

(20) Qiu, H.; Gao, Y.; Boott, C. E.; Gould, O. E. C.; Harniman, R. L.; Miles, M. J.; Webb, S. E. D.; Winnik, M. A.; Manners, I. *Science* **2016**, *352*, 697.

(21) For recent work on the use of blends of BCPs with amorphous core-forming blocks to prepare both simple and complex assemblies see: a) Zhu, J.; Zhang, S.; Zhang, K.; Wang, X.; Mays, J. W.; Wooley, K. L.; Pochan, D. J. *Nat. Commun.* **2013**, *4*, 2297; b) Wright, D. B.; Patterson, J. P.; Pitto-Barry, A.; Lu, A.; Kirby, N.; Gianneschi, N. C.; Chassenieux, C.; Colombani, O.; O'Reilly, R. K. *Macromolecules* **2015**, *48*, 6516.

(22) He, X.; Hsiao, M.-S.; Boott, C. E.; Harniman, R. L.; Nazemi, A.; Li, X.; Winnik, M. A.; Manners, I. *Nat. Mater.* **2017**, *16*, 481.

(23) Oh, J. K. *Soft Matter* **2011**, *7*, 5096.

(24) a) Kang, N.; Perron, M.-È.; Prud'homme, R. E.; Zhang, Y.; Gaucher, G.; Leroux, J.-C. *Nano Lett.* **2005**, *5*, 315; b) Kim, S. H.; Tan, J. P. K.; Nederberg, F.; Fukushima, K.; Yang, Y. Y.; Waymouth, R. M.; Hedrick, J. L. *Macromolecules* **2009**, *42*, 25; c) Nederberg, F.; Appel, E.; Tan, J. P. K.; Kim, S. H.; Fukushima, K.; Sly, J.; Miller, R. D.; Waymouth, R. M.; Yang, Y. Y.; Hedrick, J. L. *Biomacromolecules* **2009**, *10*, 1460. d) Zhang, J.; Wang, L.-Q.; Wang, H.; Tu, K. *Biomacromolecules* **2006**, *7*, 2492; e) Fu, J.; Luan, B.; Yu, X.; Cong, Y.; Li, J.; Pan, C.; Han, Y.; Yang, Y.; Li, B. *Macromolecules* **2004**, *37*, 976; f) Chen, C.-K.; Lin, S.-C.; Ho, R.-M.; Chiang, Y.-W.; Lotz, B. *Macromolecules* **2010**, *43*, 7752; g) Miyata, T.; Masuko, T. *Polymer* **1997**, *38*, 4003; f) Iwata, T.; Doi, Y. Macromolecules 1998, 31, 2461.

(25) a) Petzetakis, N.; Dove, A. P.; O'Reilly, R. K. *Chem. Sci.* **2011**, *2*, 955; b) Sun, L.; Petzetakis, N.; Pitto-Barry, A.; Schiller, T. L.; Kirby, N.; Keddie, D. J.; Boyd, B. J.; O'Reilly, R. K.; Dove, A. P. *Macromolecules* **2013**, *46*, 9074; c) Sun, L.; Pitto-Barry, A.; Thomas, A. W.; Inam, M.; Doncom, K.; Dove, A. P.; O'Reilly, R. K. *Polym. Chem.* **2016**, *7*, 2337; d) Petzetakis, N.; Walker, D.; Dove, A. P.; O'Reilly, R. K. *Soft Matter* **2012**, *8*, 7408; e) Pitto-Barry, A.; Kirby, N.; Dove, A. P.; O'Reilly, R. K. *Polym. Chem.* **2014**, *5*, 1427.

(26) Sun, L.; Pitto-Barry, A.; Kirby, N.; Schiller, T. L.; Sanchez, A. M.; Dyson, M. A.; Sloan, J.; Wilson, N. R.; O'Reilly, R. K.; Dove, A. P. *Nat. Commun.* **2014**, *5*, 5746.

(27) Wang, Z.; Cao, Y.; Song, J.; Xie, Z.; Wang, Y. *Langmuir* **2016**, *32*, 9633.

(28) Inam, M.; Cambridge, G.; Pitto-Barry, A.; Laker, Z. P. L.; Wilson, N. R.; Mathers, R. T.; Dove, A. P.; O'Reilly, R. K. *Chem. Sci.* **2017**, *8*, DOI: 10.1039/C7SC00641A.

(29) a) Hu, Z.; Fan, X.; Wang, H.; Wang, J. *Polymer* **2009**, *50*, 4175; b) Hu, Z.; Fan, X.; Zhang, G. *Carbohydrate Polymers* **2010**, *79*, 119.

(30) a) Rizis, G.; van de Ven, T. G. M.; Eisenberg, A. *Angew. Chem. Int. Ed.* **2014**, *53*, 9000; b) Rizis, G.; van de Ven, T. G. M.; Eisenberg, A. *ACS Nano* **2015**, *9*, 3627; c) Cambridge, G.; Gonzalez-Alvarez, M. J.; Guerin, G.; Manners, I.; Winnik, M. A. *Macromolecules* **2015**, *48*, 707.

(31) a) O'Reilly, R. K.; Hawker, C. J.; Wooley, K. L. *Chem. Soc. Rev.* **2006**, *35*, 1068; b) Rupar, P. A.; Cambridge, G.; Winnik, M. A.; Manners, I. *J. Am. Chem. Soc.* **2011**, *133*, 16947; c) Thurmond, K. B.; Kowalewski, T.; Wooley, K. L. *J. Am. Chem. Soc.* **1997**, *119*, 6656; d) Guo, A.; Liu, G.; Tao, J. *Macromolecules* **1996**, *29*, 2487.

(32) Qiu, H.; Du, V. A.; Winnik, M. A.; Manners, I. *J. Am. Chem. Soc.* **2013**, *135*, 17739.

(33) Wang, X.; Liu, K.; Arsenault, A. C.; Rider, D. A.; Ozin, G. A.; Winnik, M. A.; Manners, I. *J. Am. Chem. Soc.* **2007**, *129*, 5630.

(34) Gadt, T.; Ieong, N. S.; Cambridge, G.; Winnik, M. A.; Manners, I. *Nat. Mater.* **2009**, *8*, 144.

(35) (a) Gilroy, J. B.; Rupar, P. A.; Whittell, G. R.; Chabanne, L.; Terrill, N. J.; Winnik, M. A.; Manners, I.; Richardson, R. M. *J. Am. Chem. Soc.* **2011**, *133*, 17056; (b) Hsiao, M.-S.; Yusoff, S. F. M.; Winnik, M. A.; Manners, I. *Macromolecules* **2014**, *47*, 2361.

Table of Contents